Article

Discovery Medicine 2024; 36(180): 100–112
https://doi.org/10.24976/Discov.Med.202436180.9

Investigate the Therapeutic Effect of Ibandronate Sodium on Knee Osteoarthritis Based on TLRs/MyD88/NF-κB Signaling Pathway *in Vitro* and *in Vivo*

Mingxing Luo[1], Qingze Wang[1], Junguo Bao[1,*]

[1]Department of Orthopedics, Ningbo Hangzhou Bay Hospital, 315336 Ningbo, Zhejiang, China
*Correspondence: drbaojunguo@163.com (Junguo Bao)
Published: 20 January 2024

Background: For decades, bisphosphonates have primarily found application in clinical practice for the treatment and prevention of bone metastases associated with malignant tumors and various bone metabolic disorders. However, third-generation bisphosphonates like ibandronate have demonstrated significant utility in addressing conditions like osteoporosis (OA) and other bone metabolism-related ailments. Ibandronate, distinguished by its high effectiveness, low toxicity, and ease of administration, has garnered attention for its potential applications in the treatment of rheumatoid arthritis, OA, and orthopedic concerns. In recent years, the utilization of ibandronate sodium in these contexts has sparked considerable interest. Research has pointed to a possible connection between ibandronate and the Toll-like receptors (TLRs), myeloid differentiation factor 88 (MyD88), and nuclear factor-κB (NF-κB) signaling pathway, particularly in the context of inflammation and immunological regulation. Consequently, this study is designed to investigate the therapeutic impact of ibandronate on *in vitro* and *in vivo* models of knee osteoarthritis, while also delving into its influence on the TLRs/MyD88/NF-κB pathway.

Method: Various dosages of ibandronate sodium, including low (10 g/kg), medium (20 g/kg), and high (30 g/kg), were administered following the establishment of both *in vivo* and *in vitro* models of knee osteoarthritis (KOA). Post-intervention, an in-depth quantitative analysis of bone tissue microstructure was conducted. The morphology of articular cartilage tissue was observed *in vivo*, and the modified Mankin score was subsequently calculated. In the *in vitro* setting, cartilage was entirely isolated, and mRNA and total protein were extracted to measure the expression levels of TLR4, MyD88, and NF-κB at both the mRNA and protein levels. Furthermore, the study explored the effects of Interleukin-1 beta (IL-1β) on cell proliferation, apoptosis, stromal decomposition enzyme activity, ossification, and the expression of TLR4, MyD88, and NF-κB.

Result: In the results of the *in vivo* experiments, several noteworthy findings emerged. The knee curvature, gait score, Mankin score, pathological knee joint injury degree, cartilage protein loss, and trabecular separation within the model group exhibited significant elevations compared to both the sham operation group and the blank control group ($p < 0.05$). Conversely, bone density, bone volume fraction, and trabecular thickness in the model group displayed lower values in comparison to the sham operation and blank control groups ($p < 0.05$). Following the administration of ibandronate sodium, there was a progressive improvement in these parameters, with the medium and high-dose groups demonstrating the most favorable outcomes ($p < 0.05$). Additionally, the model group exhibited the highest expression levels of TLR4, MyD88, and NF-κB, while the ibandronate sodium intervention group displayed reduced expression levels of these markers, with the high-dose group registering the most significant changes ($p < 0.05$). Turning to the *in vitro* experiments, it was observed that the cell proliferation capacity and ossification degree of the IL-1β-induced group experienced declines, concomitant with an increase in stromal decomposition enzyme activity and cell apoptosis rate ($p < 0.05$). However, post-intervention with ibandronate sodium, all these indicators gradually returned to normal, with the medium-dose group exhibiting the most notable improvements. The expression levels of TLR4, MyD88, and NF-κB in the IL-1β-induced group showed an increase, while the expression levels in the ibandronate sodium intervention group displayed a decrease, particularly in the high-dose group ($p < 0.05$).

Conclusions: Ibandronate sodium demonstrates a protective effect on articular chondrocytes and exhibits the potential to decelerate the pathological progression of knee osteoarthritis (KOA) in rats. This mechanism is likely achieved through the inhibition of the TLRs/MyD88/NF-κB signaling pathway.

Keywords: ibandronate sodium; knee osteoarthritis; TLRs/MyD88/NF-κB; articular chondrocyte

Introduction

Osteoarthritis (OA) stands as the most prevalent degenerative joint ailment encountered in clinical practice, ranking among the foremost causes of adult disability and congenital abnormalities [1,2]. The etiology of knee osteoarthritis (KOA) remains relatively obscure, and available diagnostic methods are limited, leading to a low success rate in treating KOA. The primary objective in managing KOA revolves around alleviating pain symptoms and controlling disease progression. Nonetheless, a significant proportion of drugs commonly employed for this purpose tend to induce adverse reactions in the gastrointestinal, cardiovascular, and renal systems, thus lowering patient tolerance [3,4]. Currently, there exist some contentious perspectives regarding the treatment of KOA. Firstly, clinical attention to KOA remains inadequate, particularly in terms of fostering enthusiasm for additional drug research and development. Secondly, KOA is frequently oversimplified as a mere joint ailment, often disregarding its potential repercussions on other bodily systems, such as cardiovascular and psychological health. Thirdly, the dearth of research into the pathophysiology of KOA contributes to a lack of comprehensive understanding of the condition, which, in turn, impacts the clinical benefits for patients.

In recent times, a cadre of academics has advanced the proposition that the Toll-like receptors (TLRs), myeloid differentiation factor 88 (MyD88), and the transcription factor nuclear factor-κB (NF-κB) signaling pathway constitute a pivotal route governing the body's innate immune response. This pathway also serves as a crucial bridge between the innate and acquired immune responses, exerting a substantial influence on the development of inflammatory diseases [5–9]. Research has underscored the abnormal activation of TLRs/MyD88/NF-κB in conditions such as systemic lupus erythematosus, inflammatory bowel disease, asthma, and other autoimmune and inflammatory ailments [10–12]. Furthermore, studies have elucidated the role of the TLRs/MyD88/NF-κB signaling pathway in regulating inflammation in rheumatoid arthritis [13]. Consequently, the modulation of TLRs/MyD88/NF-κB signaling pathway activation has emerged as a promising avenue for clinical research with the aim of treating knee osteoarthritis.

Bisphosphonate drugs have been in clinical use for several decades, primarily employed for the prevention and treatment of bone metastasis in malignant tumors and various bone metabolic disorders. The third generation of bisphosphonates, which includes ibandronate sodium, stands out for its commendable effectiveness, low toxicity, and user-friendly administration. Notably, the US Food and Drug Administration (FDA) has granted approval for the quarterly administration of ibandronate sodium injection in the treatment of postmenopausal osteoporosis in women, marking a significant advancement that greatly enhances patient tolerance [14]. Existing studies have reported the utilization of ibandronate sodium in osteoporosis treatment, showing promising results [15,16].

In the realm of clinical practice, observations have revealed that ibandronate sodium not only impedes bone absorption but also influences the activation of various cytokines and signaling pathways. It fosters chondrocyte proliferation, suppresses synovial inflammation, and has thus attracted significant attention in its application to the treatment of conditions such as rheumatoid arthritis, OA, and orthopedic concerns [17,18]. As a bisphosphonate, ibandronate sodium primarily curtails bone loss by inhibiting bone resorption, consequently preserving bone density. Given the interplay between bone metabolism and the immune system, it is plausible that the impact of ibandronate sodium is linked to the regulation of the TLR4/MyD88/NF-κB signaling pathway. Consequently, ibandronate sodium may exert a certain influence on bone metabolism by modulating the immune system's inflammatory response. However, the specific mechanisms of action and their ramifications warrant further validation and exploration through laboratory studies and clinical practice.

This study delved into the precise mechanism of ibandronate sodium concerning KOA, specifically within the context of the aforementioned TLRs/MyD88/NF-κB signaling pathway, and ibandronate sodium's role in the initiation and progression of inflammatory disorders. The research examined the therapeutic impact of ibandronate sodium on KOA, both *in vivo* and *in vitro*, while concurrently investigating the molecular mechanism associated with the TLRs/MyD88/NF-κB signaling pathway. These findings provide experimental support for the development of clinical drugs for KOA and the utilization of ibandronate sodium in the field of orthopedics.

Methods

Animal Origin

Animal experiments were conducted in compliance with the ethical standards and procedures outlined by the Experimental Animal Ethics Committee of our hospital. A total of thirty 12-week-old female Sprague-Dawley (SD) rats, with an average body mass of (220.54 $\pm$ 10.64) g, were sourced for the study. These rats were procured from Hunan Lake Jingda Laboratory Animal Co., LTD. (Changsha, Hunan, China), under license number SYXK(Xiang)2021-0002. To acclimate the animals, they were subjected to a 12-hour light/dark cycle and housed in an environment with a temperature of approximately 24 ℃ and a humidity level of 50% for one week prior to the commencement of the experiment. All animal experiments strictly adhered to the "Guidelines for the Care and Use of Laboratory Animals" published by the National Academy of Sciences.

Drug Administration and Grouping in Animal Modeling

The experimental rats were divided into six groups, each comprising five rats: a blank control group, a sham operation group, a model group, and three experimental groups (low, medium, and high dosage). In the model and experimental groups, a knee osteoarthritis model was induced in the rats through the following procedure: After administering an intraperitoneal injection of 1% pentobarbital sodium (40 mg/kg, Ayrton Saunders, Cheshire, UK), the rats were immobilized on the operating table. The right medial knee joint was fully exposed, and the anterior cruciate ligament was surgically severed. The incision was subsequently sutured, and post-operative care involved standard feeding and the application of antibiotics to prevent wound infection. Both the sham operation group and the model group underwent the same surgical procedure, with the exception that the anterior cruciate ligament was not severed. The blank control group received no treatment whatsoever. In terms of administration, one week after surgery, rats in the experimental groups were subcutaneously injected with ibandronate sodium (10, 20, 30 mg/kg) [19] (H20010432, Shijiazhuang Kaida Biological Engineering Co., LTD., Hebei, China) once a week for a duration of 12 weeks. Meanwhile, the rats in the blank group, sham surgery group, and model group received an equivalent volume of regular saline via intraperitoneal administration.

Pain Assessment Methods

To evaluate exercise-induced nociception in each group of rats, knee bending tests were employed. During these tests, any squeak and/or struggle responses observed in reaction to five alternating knee flexion and extension movements (performed within the physiological limits of knee mobility) were meticulously recorded. The scores were assigned as follows: 0 indicating no response, 0.5 reflecting an attempt to achieve maximum flexion/extension, 1 signifying an attempt at moderate flexion/extension or vocalization while achieving maximum flexion/extension, and 2 denoting vocalizations during moderate flexion/extension. The sum of these responses, with a maximum total of 20, yielded the knee bend score. Gait analysis was conducted by applying ink to the undersides of the rats' hind feet and guiding them to walk along the full length of a sheet of paper. This allowed for a comparison of the footprints of the injected leg with those of the uninjected leg, thereby enabling an assessment of weight distribution during exercise.

Microscopic Computed Tomography Analysis

Following the intervention, the rats were humanely euthanized using an overdose of 4% pentobarbital (40 mg/kg). The entire knee segment was then harvested for microcomputed tomography (μCT) analysis, utilizing the VivaCT40 system (Sanco Medical AG, Bruttisellen, Switzerland) with a resolution of 35 mm. A rectangular target region measuring 2 mm in length, 1 mm in width, and 0.5 mm in depth was carefully positioned within the subchondral bone at both the medial and lateral epiphyses of the tibia. Trabecular indices were quantified, encompassing bone density, bone volume fraction, trabecular number, trabecular thickness, and trabecular separation.

Histological Score

Tissue sections were subject to observation using hematoxylin and eosin (HE) staining (G1120, Solarbio, Beijing, China) and Safranin O staining (S8020, Solarbio, Beijing, China) under a light microscope. HE staining was employed to assess the cartilage tissue structure, chondrocytes, and subchondral bone. Safranin-O staining, on the other hand, was utilized to detect changes in proteoglycan levels. The sections, stained with both HE and Safranin-O, were scored in accordance with Mankin's histological grading method for osteoarthropathy [20], with three fields selected for evaluation within each section.

Cell Culture and Grouping

Human chondrocytes (CP-H107, Procell, Wuhan, China) were cultured in a specialized and complete human cartilage cell culture medium, which contained essential components such as fetal bovine serum (FBS), growth additives, Penicillin, Streptomycin, and others (CM-H107, Procell, Wuhan, China). This cell culture was maintained at 37 °C within a 5% CO_2 cell incubator, with regular medium changes every 2–3 days. The chondrocytes were categorized into distinct groups, namely the blank control group, the Interleukin-1 beta (IL-1β) treatment group (10 ng/mL) using IL-1β (90105ES08, Yisheng Biotechnology (Shanghai) Co., LTD., Shanghai, China), and the ibandronate sodium group. In the ibandronate group, cells were exposed to 10 ng/mL IL-1β followed by treatment with ibandronate sodium (20 μg/mL). All cells employed in this study underwent short tandem repeat (STR) identification and were tested for mycoplasma presence (verified through PCR) to ensure their authenticity and to confirm the absence of mycoplasma and other pathogenic bacterial infections. All experimental procedures strictly adhered to the principles of aseptic techniques.

CCK-8 Experiment

Using the cell counting kit-8 (CCK-8) (556545, Huinuo Biomedical Technology Hangzhou Co., LTD., Hangzhou, China), CCK-8 reagent was prepared and utilized to assess the proliferative capacity of cells in various groups, including the blank control group, the IL-1β treatment group (10 ng/mL), and different ibandronate sodium concentrations (2, 5, 10, 20, 40 μg/mL). This evaluation aimed to determine the optimal intervention concentration of ibandronate sodium. The cells were combined with the

Table 1. Primer sequence.

Name	Forward primer	Reverse primer
TLR4 (tissue)	5′-GGACCTGAGCTTTAATCCC-3′	5′-GGACCTGAGCTTTAATCCC-3′
TLR4 (cell)	5′-AGCCTGGGAGAGGAGGAAAG-3′	5′-CCTTGGGGAAGGTGGAAG-3′
MyD88 (tissue)	5′-CAGCATTGAGGAGGATTGC-3′	5′-GGGACACTGCTGTCTACAG-3′
MyD88 (cell)	5′-TTGCCTGTGGACCTGAACTG-3′	5′-CCAGGTTCTGCACCTGACCT-3′
NF-κB (tissue)	5′-GGGAGAGGCGGTGGAAGTGT-3′	5′-GGTTCCAGGTGAGGGTAGGG-3′
NF-κB (cell)	5′-GGAGGAGGAGGAAGGAGGAAG-3′	5′-CTTGAGGGGCTTTTGAGGAA-3′
GAPDH (tissue)	5′-TCAAGATCATCAGCAATGCC-3′	5′-CGATACCAAAGTTGTCATGGA-3′
GAPDH (cell)	5′-GAAGGTGAAGGTCGGAGT-3′	5′-GAAGATGGTGATGGGATTTC-3′

NF-κB, nuclear factor-κB; *TLR*, Toll-like receptors; *MyD88*, myeloid differentiation factor 88; *GAPDH*, glyceraldehyde-3-phosphate dehydrogenase.

CCK-8 reagent and subsequently incubated in the cell incubator for 12, 24, 48, and 72 hours. Following incubation, the absorbance at 450 nm was measured, and the cell proliferation rate was computed using the following formula: Cell Proliferation Rate (%) = (OD (experimental group) − OD (control group)/OD (control group)) × 100%, optical density (OD).

Flow Cytometry Experiment

The cells were removed from the medium, and fixation and osmotic reagents were applied to immobilize the cells and facilitate the penetration of fluorescent dye into their interior. Propidium Iodide (PI, HY-D0815, MedChemExpress, Shanghai, China) was used to stain the cells, and cell analysis was conducted using flow cytometry (Attune™, Thermo Fisher, Waltham, MA, USA). Apoptotic cells were identified based on the fluorescence intensity and wavelength of the stain within the cells, and the percentage of apoptotic cells was subsequently calculated. The formula used for calculating the percentage of apoptotic cells is as follows: Percentage of Apoptotic Cells (%) = (number of apoptotic cells/total number of cells) × 100%.

ELISA Experiment

The activity levels of matrix-degrading enzymes (Matrix metalloproteinases (MMPs), F10343-B, Fankew, Shanghai, China; A Disintegrin and Metalloproteinase with Thrombospondin motifs (ADAMTS), F111831-B, Fankew, Shanghai, China) were assessed through enzyme-linked immunosorbent assays (ELISA). In this process, the antigen or antibody solution to be detected is introduced into the wells of a microplate for incubation, allowing the antigen or antibody to adhere to the microplate's bottom. Subsequently, a blocking agent was added to minimize non-specific binding, followed by the incubation of an enzyme-labeled antibody. An enzyme substrate was then introduced, forming a bond with the enzyme-labeled antibody. After a designated incubation period, the absorbance at 450 nm was measured using a spectrophotometer. The concentration of target molecules in the sample to be analyzed was determined either through the use of a standard curve or a computational method.

Alkaline Phosphatase (ALP) Dye

The alkaline phosphatase staining solution (G1480, Solarbio, Beijing, China) was prepared for use. The culture medium from the cultivated cells was aspirated, and the prepared Alkaline Phosphatase (ALP) staining solution was individually added to ensure even distribution across the cells in each group. The Petri dish was then returned to the cell incubator and allowed to incubate for 30 minutes. Subsequently, a gentle buffer solution was employed to wash away any unbound stain. ALP substrate was introduced to react with the ALP within the cells. Following the reaction, a buffer solution was employed to halt the process, and the cells were examined under a microscope to observe the location and distribution of alkaline phosphatase activity within the cells. Cells exhibiting ALP activity might display stained colors or deposits.

Quantitative Real Time Polymerase Chain Reaction (qRT-PCR)

For the collection of cell and tissue samples, total RNA extraction was carried out using Trizol reagent (NEP019-1, Dingguo, Beijing, China). Subsequently, reverse transcription was performed to convert the RNA into cDNA. The PCR reaction mixture was then prepared, which included appropriate concentrations of primers, probes, cDNA/DNA, buffers, and polymerase. The temperature cycling program for the PCR instrument was established. Using glyceraldehyde-3-phosphate dehydrogenase (GAPDH) as an internal reference, the expression levels of TLR4, MyD88, and NF-κB were quantitatively determined using the $2^{-\Delta\Delta Ct}$ method [21]. The primer sequences (Table 1) were synthesized by Shanghai Shenggong Biotechnology Co., LTD. (Shanghai, China).

Western Blot

Total protein was extracted from cells and tissues, and bicinchoninic acid (BCA) quantitative protein analysis was performed. The subsequent steps included gel preparation with a 10% separation gel and a 5% concentration gel, electrophoresis (maintained at a constant pressure of 75 mV for approximately 130 minutes), gel cutting, membrane trans-

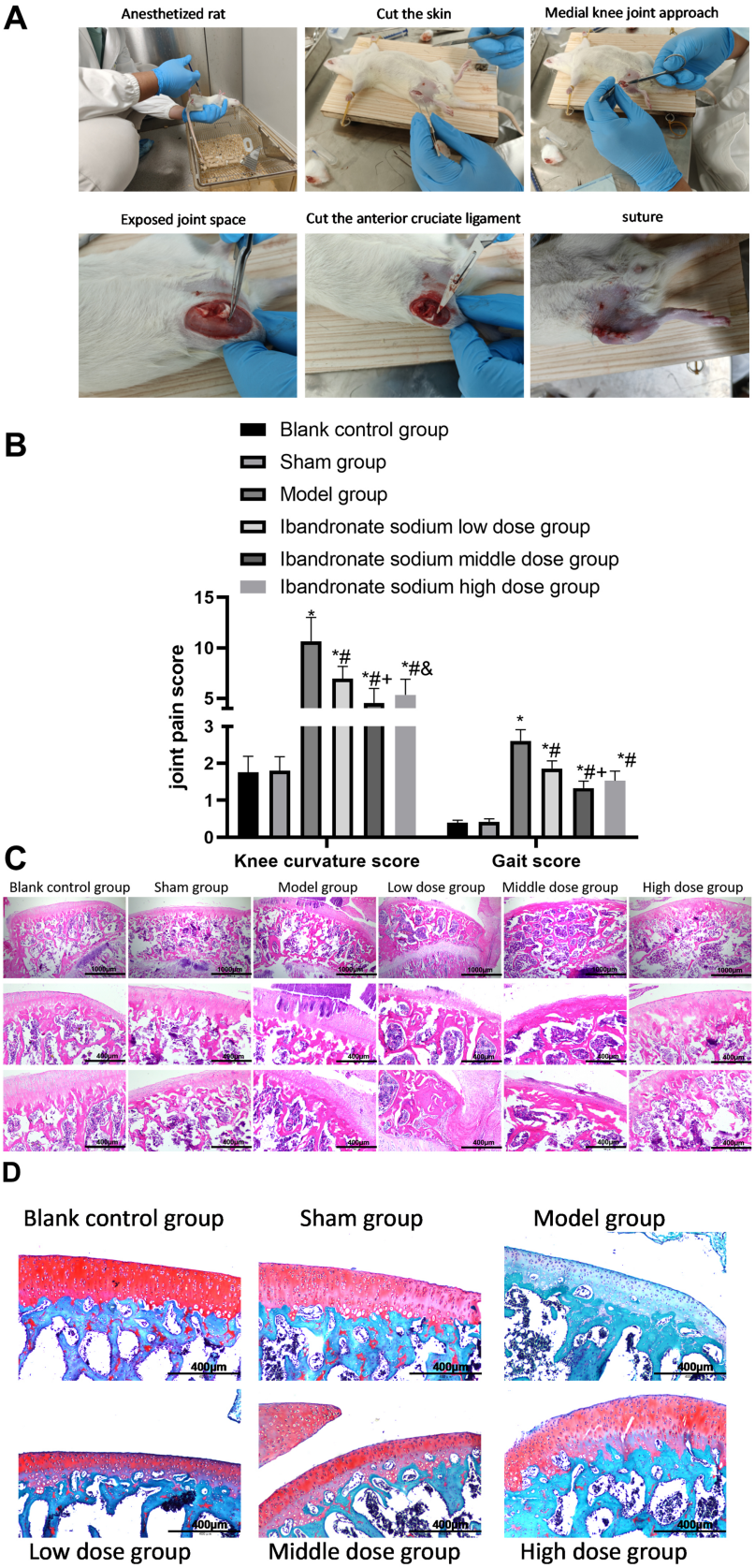

Fig. 1. Establishment of knee osteoarthritis (KOA) rat model and pathological changes (n = 5). (A) KOA Model establishment. (B) Joint pain detection. (C) Hematein Eosin dye (400 μm). (D) Safranin-O dye (400 μm). *$p < 0.05$ vs Sham group, #$p < 0.05$ vs Model group, +$p < 0.05$ vs Ibandronate sodium low dose group, &$p < 0.05$ vs Ibandronate sodium middle dose group.

fer (conducted at a constant current of 300 mA), closure (lasting 90 minutes at 25 °C), and incubation with primary antibodies (TLR4, A5258, 1:1000; Abclonal, Wuhan, China; MyD88, A0980, 1:100; Abclonal, Wuhan, China; NF-κB, 1:100; A6667, Abclonal, Wuhan, China) for 16 hours at 4 °C. Subsequently, goat anti-rabbit secondary antibody (1:3000) was incubated at 25 °C. The nitrocellulose filter membrane (NC) film was treated with electrochemiluminescence (ECL) chemiluminescence solution (CSB-K11714CL, Dingguo, Beijing, China) and incubated for one minute. Once the liquid was completely absorbed by the filter paper, it was exposed for one to twenty minutes to the X-ray film within a dark box before being developed. Protein gray values were assessed using Image J (V1.8.0.112, NIH, Madison, WI, USA), and the gray value was calculated as follows: Gray value = (sum of pixel values in this area)/(Number of pixels in this area).

Statistical Analysis

The statistical analysis was conducted using SPSS 26.0 (SPSS, Inc., Chicago, IL, USA). Measurement data were presented as Mean $\pm$ SD (standard deviation). One-way analysis of variance was employed for comparisons among different groups, and for pairwise comparisons of variances, either the least significant difference (LSD) or Students Newman-Krue (SNK) technique was utilized. The significance level for this experiment was set at 0.05.

Result

Establishment of KOA Rat Model and Pathological Changes

In Fig. 1A, the image illustrates the mold's formation. Findings from joint pain detection indicated that the knee curvature and gait scores in the model group were significantly higher than those in the sham surgery group ($p < 0.05$). Additionally, the knee joint curvature and gait scores in the low, medium, and high-dose groups were all lower than those in the model group. Notably, the medium-dose group demonstrated the lowest scores (Fig. 1B; $p < 0.05$). HE staining revealed that the cartilage structure in groups without modeling and those that underwent sham surgery remained normal and had a higher cell count. In contrast, the model group displayed a dispersed cartilage structure, a decreased number of cells, and an infiltration of inflammatory cells. The ibandronate low, medium, and high-dose groups exhibited an improved cartilage structure with more cells and fewer inflammatory cells compared to the model group (Fig. 1C).

Safranin-O staining depicted that cartilage proteoglycan in the blank control group was uniformly stained with red dye, while the subchondral bones and bone trabeculae appeared green. The sham surgery group showed no loss of cartilage proteoglycan, although the staining was lighter. In the model group, the entire cartilage proteoglycan layer showed destaining. In the low, medium, and high-dose ibandronate sodium groups, the staining of cartilage proteoglycans was uneven, pale, and some areas displayed destaining (Fig. 1D).

Ibandronate Sodium can Stabilize the Mankin Score and Trabecular Bone Indexes of Patients in Each Group

The Mankin scores in the model group were significantly higher than those in the sham surgery group, while the Mankin scores in the low, medium, and high-dose ibandronate sodium groups were notably lower than those in the model group (Fig. 2A; $p < 0.05$). Comparing the model group with the sham surgery and blank control groups, the model group exhibited greater trabecular separation and lower bone mineral density, bone volume percentage, and trabecular thickness ($p < 0.05$). In contrast, the low, medium, and high concentrations of ibandronate sodium groups demonstrated increased bone density, bone volume percentage, and trabecular thickness compared to the model group, with lower trabecular separation (Fig. 2B,C; $p < 0.05$).

Ibandronate Sodium can Reduce the Expression Levels of TLR4, MyD88 and NF-κB

The mRNA and protein expression levels of TLR4, MyD88, and NF-κB in the model group were significantly higher than those in the sham surgery and blank control groups, while these expression levels were notably lower in the low, medium, and high-dose ibandronate sodium groups (Fig. 3A,B; $p < 0.05$).

Ibandronate Sodium can Improve the Reduction of Cell Proliferation after Interleukin-1 Beta (IL-1β) Induction and Decrease Apoptosis

The results of the CCK-8 experiment revealed that the cell proliferation rate in the IL-1β group was significantly lower than that in the blank control group ($p < 0.05$). However, the cell proliferation rate increased following the intervention of ibandronate sodium, with 20 µg/mL showing the most substantial effect (Fig. 4A; $p < 0.05$). Consequently, 20 µg/mL was selected as the optimal intervention dose of ibandronate sodium for subsequent experiments. Observations of cell morphology indicated that chondrocytes in the blank control group were uniformly scattered, exhibited a spindle shape, and had a rapid growth rate after adhesion. In contrast, chondrocytes in the IL-1β group displayed changes to a long spindle shape or irregular shape after adhesion, slower growth, and an extended passage time. Following the intervention of the ibandronate sodium group, cell morphology gradually returned to normal, and the passage time was shortened (Fig. 4B). Flow cytometry analysis demonstrated that the apoptosis rate in the IL-1β group was significantly higher than that in the blank control group ($p < 0.05$). However, in comparison to the IL-1β group, the ibandronate sodium group exhibited a decreased apoptosis rate (Fig. 4C; $p < 0.05$).

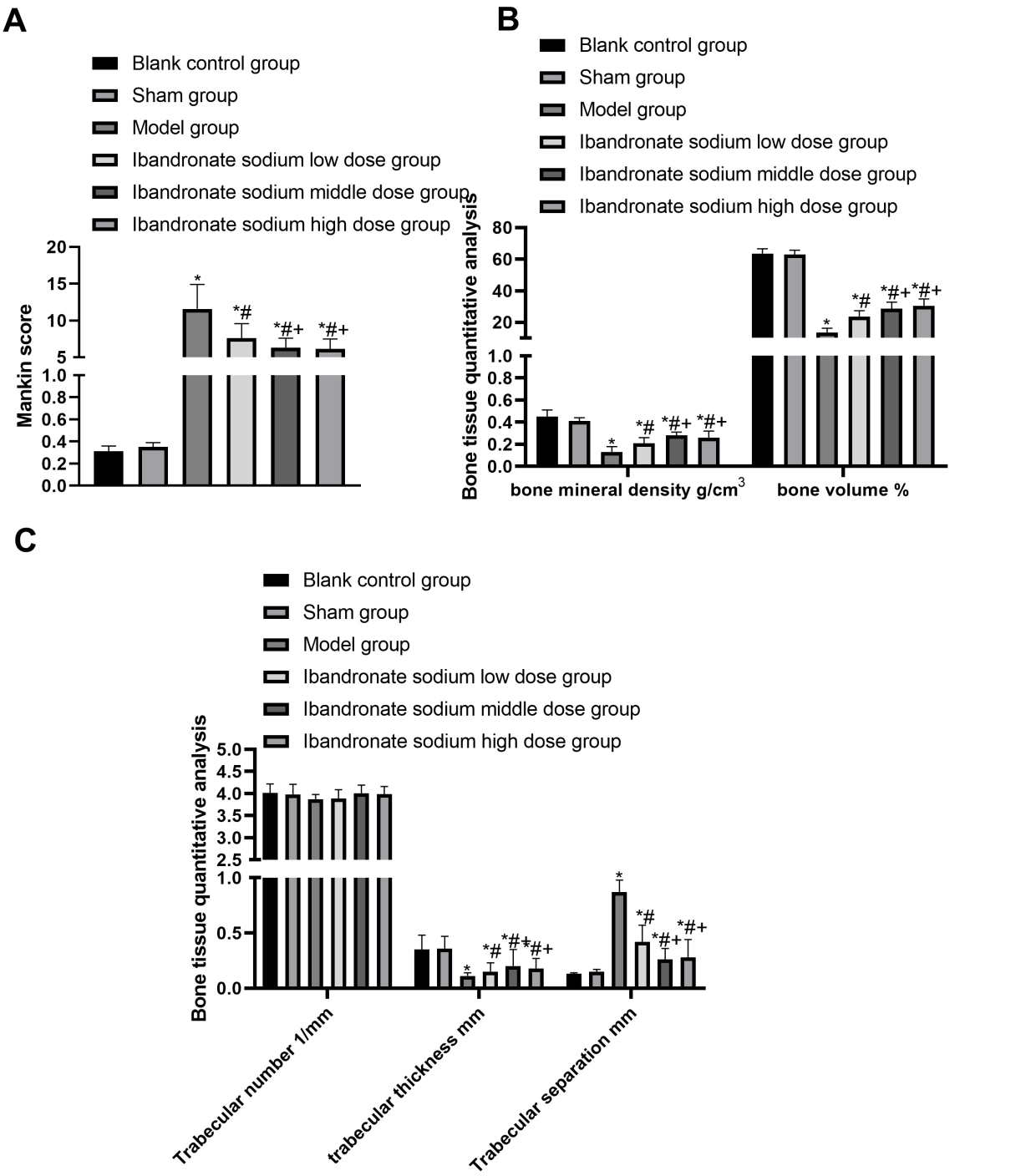

Fig. 2. Ibandronate sodium can stabilize the Mankin score and trabecular bone indexes of patients in each group (n = 5). (A) Mankin score. (B,C) Bone tissue quantitative analysis. *$p < 0.05$ vs Sham group, #$p < 0.05$ vs Model group, +$p < 0.05$ vs Ibandronate sodium low dose group.

Ibandronate Reduces IL-1β-Induced Matrix Decomposing Enzyme Activity and Increases Ossification and Calcification

Based on the ELISA data, the activities of MMPs and ADAMTS in the IL-1β group were significantly elevated in comparison to the blank control group, whereas the activities of MMPs and ADAMTS were reduced and increased, respectively, following intervention with ibandronate sodium (Fig. 5A; $p < 0.05$). The ALP staining results indicated that the IL-1β group had a low number of ALP-positive cells and exhibited shallow staining, while the ibandronate sodium intervention resulted in an increased number of ALP-positive cells with deeper staining (Fig. 5B).

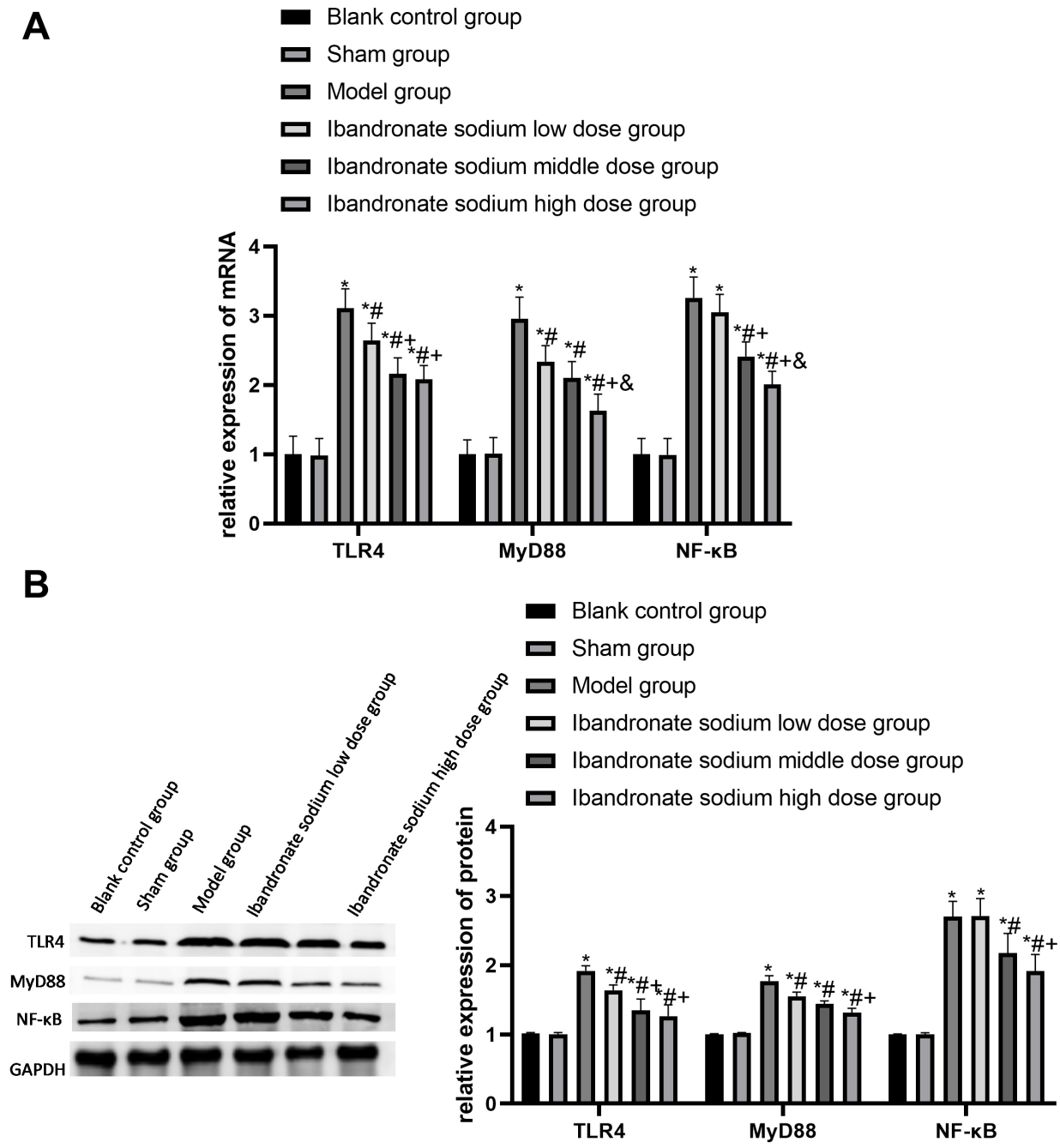

Fig. 3. Ibandronate sodium can reduce the expression levels of TLR4, MyD88 and NF-κB (n = 5). (A) TLR4, MyD88, and NF-κB mRNA expression levels. (B) TLR4, MyD88, and NF-κB protein expression levels. *$p < 0.05$ vs Sham group, #$p < 0.05$ vs Model group, +$p < 0.05$ vs Ibandronate sodium low dose group, &$p < 0.05$ vs Ibandronate sodium middle dose group.

Ibandronate can Reduce the Expression of TLR4, MyD88 and NF-κB in IL-1β-Induced Cells

The mRNA and protein expression levels of TLR4, MyD88, and NF-κB in the IL-1β group were significantly higher than those in the blank control group. In contrast, TLR4, MyD88, and NF-κB expression levels in the ibandronate low, medium, and high dosage groups were notably lower than those in the IL-1β group (Fig. 6A,B; $p < 0.05$).

Discussion

KOA is characterized by significant pathological features, including articular cartilage disease, bone hyperplasia, reconstruction, and synovial inflammation. These factors result in an abnormal anatomical structure and compromised functionality of the entire knee joint [22,23]. In certain cases, KOA may have advanced to a more severe stage, marked by extensive cartilage wear and prominent bone hyperplasia. While numerous treatment options are

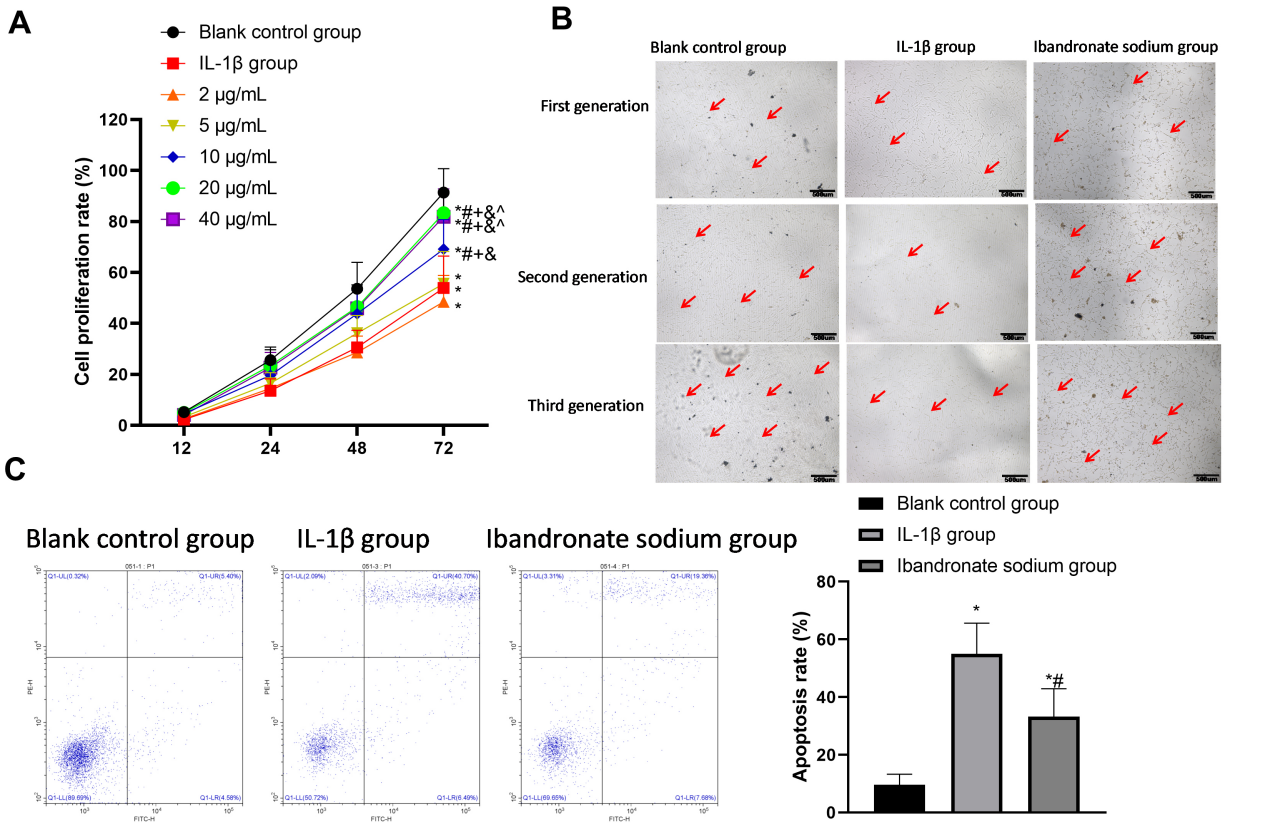

Fig. 4. Ibandronate sodium can improve the reduction of cell proliferation after Interleukin-1 beta (IL-1β) induction and decrease apoptosis (n = 3). (A) Cell proliferation rate. (B) Cell growth state (500 μm) (The arrows represent proliferating cells). (C) Cell apoptosis rate. *$p < 0.05$ vs Blank control group, #$p < 0.05$ vs IL-1β group, +$p < 0.05$ vs 2 μg/mL, &$p < 0.05$ vs 5 μg/mL, ^$p < 0.05$ vs 10 μg/mL.

available, there are instances where treatment may prove ineffective. Consequently, the discovery of new therapeutic approaches for KOA holds immense significance. Such discoveries could enhance the clinical cure rate and alleviate the condition's pathological complexities.

Bisphosphonates, a class of drugs commonly employed to manage osteoporosis and bone metastases, exert their action by inhibiting bone resorption, consequently mitigating the loss of bone tissue. Bisphosphonates are synthetic chemical compounds known for their high affinity to calcium crystals. The latest generation of these drugs, the third generation, comprises nitrogen-containing bisphosphonates with a heterocyclic structure, including ibandronate sodium and zoledronic acid. Compared to their predecessors in the first and second generations, these drugs exhibit greater potency, require lower dosages, and have significantly improved patient tolerance [24]. However, research investigating the relationship between bisphosphonates and knee osteoarthritis (KOA) remains limited.

In the earlier stages of research, Moreau *et al.* [25] established a dog model of knee osteoarthritis and observed that the first-generation bisphosphonate, Tirudronate sodium, effectively preserved calcified cartilage and subchondral bone morphology. It reduced synovial inflammatory responses and improved anatomical bone and joint lesions. In our study, we found that ibandronate sodium intervention ameliorated joint pain in arthritis model rats. It also lowered the Mankin score, reduced the degree of pathological knee joint injury, and mitigated cartilage protein loss. Additionally, it brought about alterations in bone density, bone volume fraction, bone trabecular thickness, and bone separation in knee joints. These results suggest that ibandronate sodium can decrease bone resorption in the early stages of knee osteoarthritis, leading to an increase in the number and density of bone trabeculae. This, in turn, restores the biomechanical effect of subchondral bone and potentially delays or treats KOA. The mechanism behind this may be attributed to ibandronate belonging to the class of drugs called bisphosphonates. These drugs hinder the activity of bone-damaging osteoclasts and protect the bone surrounding the joint. Given that abnormal bone metabolism is a common feature in OA, and ibandronate may enhance joint function by maintaining joint stability.

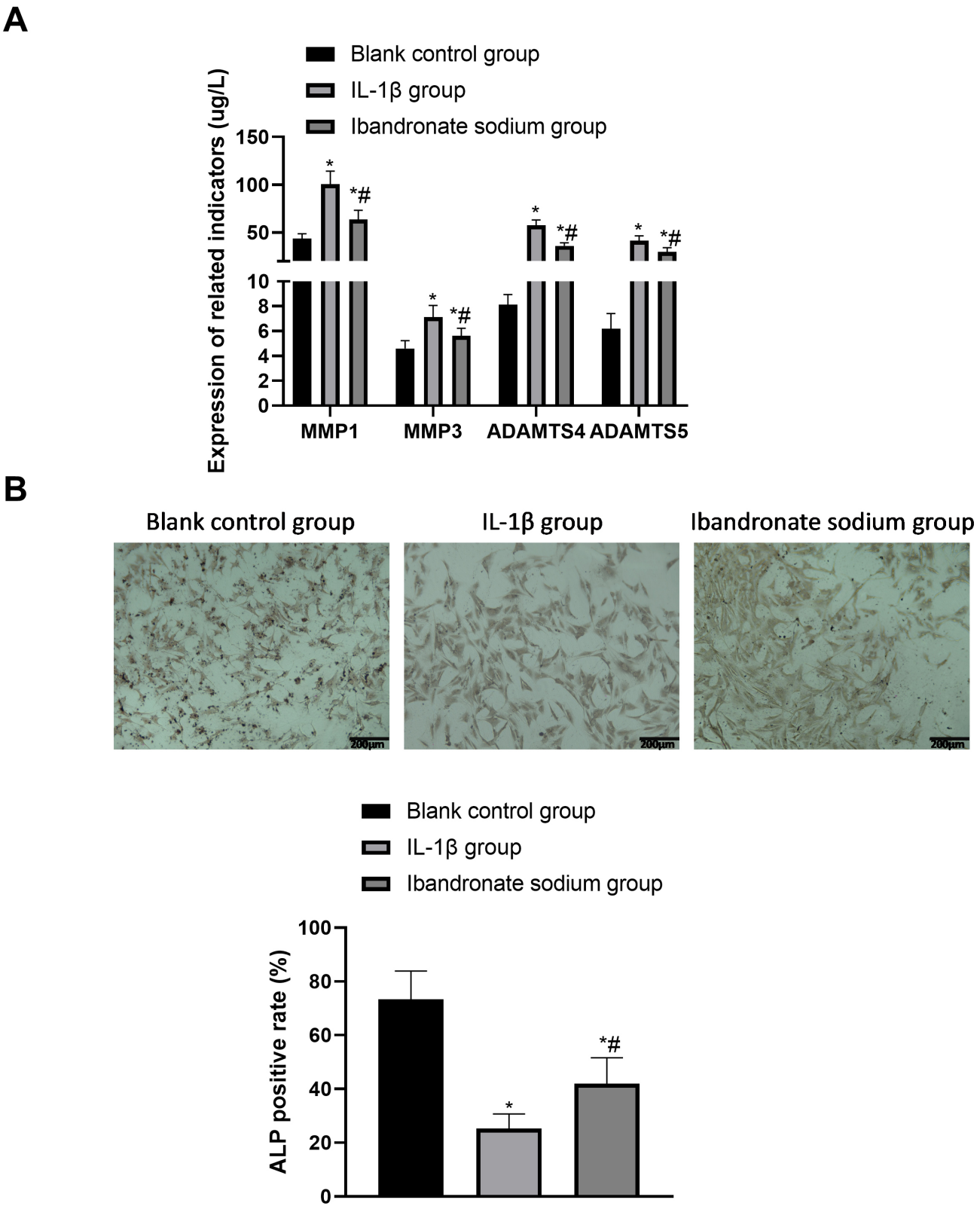

Fig. 5. Ibandronate reduces IL-1β-induced matrix decomposing enzyme activity and increases ossification and calcification (n = 3). (A) The activities of Matrix metalloproteinases (MMPs) and A Disintegrin and Metalloproteinase with Thrombospondin motifs (ADAMTS). (B) Alkaline Phosphatase (ALP) dye (200 μm). The less brown precipitate formation, the less ALP positive cells, the less calcification; The more brown precipitates formed, the more ALP positive cells, and the more calcification. *$p < 0.05$ vs Blank control group, #$p < 0.05$ vs Interleukin-1 beta (IL-1β) group.

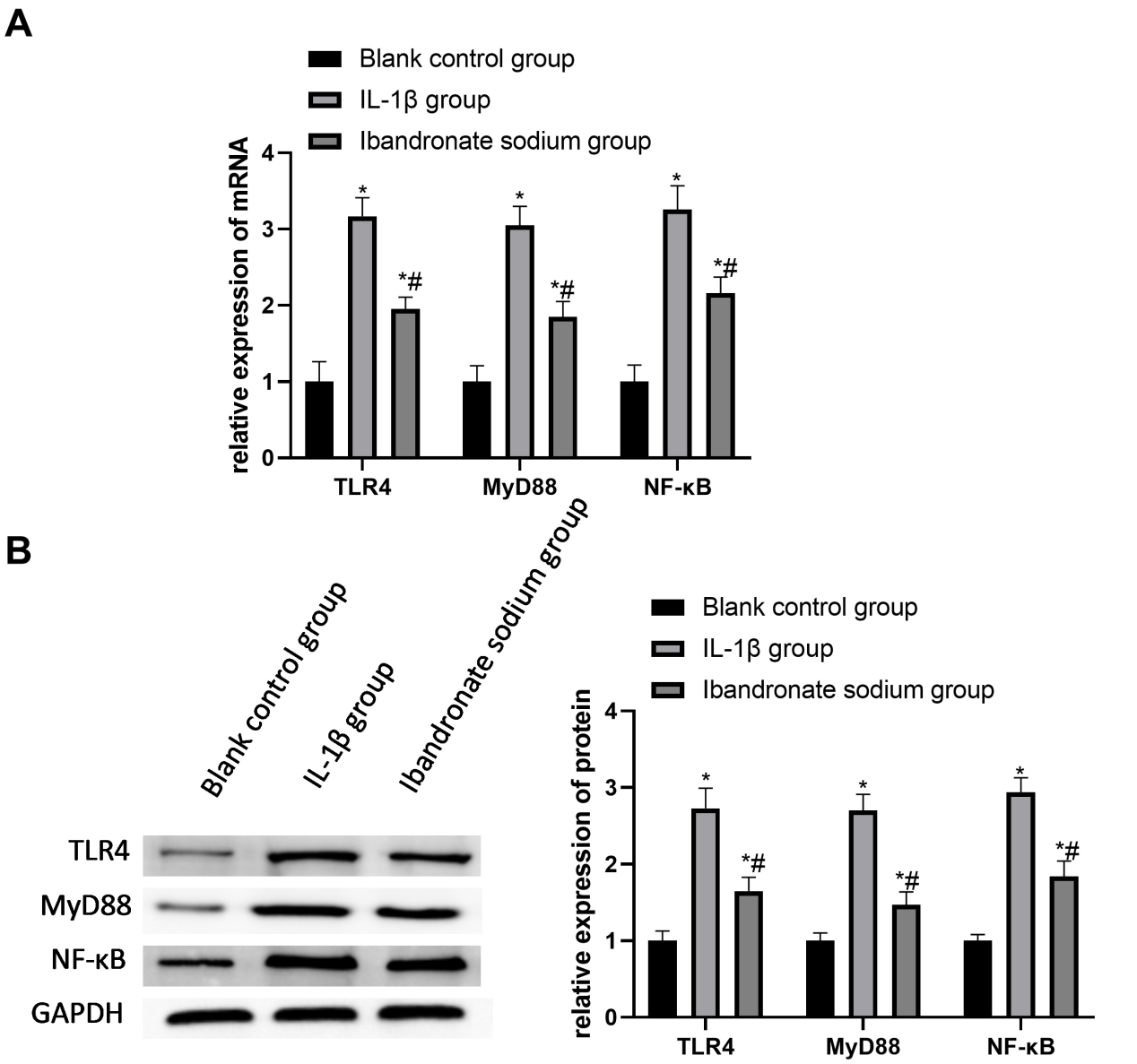

Fig. 6. Ibandronate can reduce the expression of TLR4, MyD88 and NF-κB in IL-1β-induced cells (n = 3). (A) TLR4, MyD88, and NF-κB mRNA expression levels. (B) TLR4, MyD88, and NF-κB protein expression levels. *$p < 0.05$ vs Blank control group, #$p < 0.05$ vs IL-1β group.

The pathogenesis of KOA involves mechanical changes, oxidative stress, and immune responses, which are believed to be the primary causes of cartilage degeneration and pain symptoms [26]. Research has shown that the activation of the nuclear factor-erythroid 2-related factor-2 (*Nrf2*) gene can prevent joint cartilage damage [27–30]. Studies conducted by Gu *et al.* [31] have confirmed that upregulating *TLR4* mRNA expression in chondrocytes can influence the secretion of IL-1β and type II collagen. MyD88 is a critical intermediary molecule in the signaling pathway mediated by TLRs [32,33]. However, whether MyD88 plays a downstream role in this signaling pathway, ultimately activating NF-κB and affecting the secretion of downstream cytokines, is still under investigation [34].

Numerous studies have indicated that TLRs are highly expressed in articular cartilage tissue and may play a vital role in the progression of OA. The increase in serum TLR5 levels is also associated with articular cartilage destruction to some extent [35,36]. Based on prior research, the interactions involving TLR4, MyD88, and NF-κB have implications for the immune system, inflammatory responses, and the regulation of bone metabolism. The inhibitory effect of ibandronate sodium may influence inflammatory responses and immune regulation by interacting with specific components of the TLR4/MyD88/NF-κB signaling pathway. This effect may have a regulatory impact on bone metabolism, especially in conditions involving bone diseases associated with inflammation. In our study, we observed an increase

in the expression of TLR4, MyD88, and NF-κB in the articular cartilage tissue of the animal arthritis model. After ibandronate sodium intervention, the levels of TLR4, MyD88, and NF-κB gradually decreased. These findings are in line with the previously mentioned research results and suggest that ibandronate can modulate the expression of TLR4, MyD88, and NF-κB, potentially affecting the development of OA.

Conclusions

The *in vitro* experimental results demonstrated that the IL-1β-induced group exhibited reduced cell proliferation, decreased stromal decomposition enzyme activity, impaired ossification and calcification, and a higher rate of cell apoptosis. However, following the intervention of ibandronate sodium, all these indices gradually returned to normal levels. Additionally, the increase in the expression levels of TLR4, MyD88, and NF-κB induced by IL-1β was reversed after the intervention of ibandronate sodium. These findings strongly suggest that ibandronate sodium can protect articular chondrocytes by inhibiting the expression of TLR4, MyD88, and NF-κB, consequently reducing the pathological progression of KOA in rats. This protective effect on articular chondrocytes, combined with its impact on various aspects of KOA pathology, underscores the potential of ibandronate sodium as a valuable therapeutic option for KOA.

Availability of Data and Materials

All data included in this study are available upon request by contact with the corresponding author.

Author Contributions

ML and QW designed the research study. QW and JB performed the research. ML and JB collected and analyzed the data. ML and QW have been involved in drafting the manuscript and all authors have been involved in revising it critically for important intellectual content. All authors give final approval of the version to be published. All authors have participated sufficiently in the work to take public responsibility for appropriate portions of the content and agreed to be accountable for all aspects of the work in ensuring that questions related to its accuracy or integrity.

Ethics Approval and Consent to Participate

Animal experiments shall be approved and recorded by the experimental Animal Ethics Committee of Ningbo Hangzhou Bay Hospital (2021-Q35).

Acknowledgment

We would like to express our gratitude to the participants who generously gave their time and effort to make this study possible.

Funding

It is supported by Ningbo Medical Science and Technology Plan Project (2021Y80).

Conflict of Interest

The authors declare no conflict of interest.

References

[1] Katz JN, Arant KR, Loeser RF. Diagnosis and Treatment of Hip and Knee Osteoarthritis: A Review. JAMA. 2021; 325: 568–578.

[2] Molnar V, Matišić V, Kodvanj I, Bjelica R, Jeleč Ž, Hudetz D, *et al*. Cytokines and Chemokines Involved in Osteoarthritis Pathogenesis. International Journal of Molecular Sciences. 2021; 22: 9208.

[3] Figus FA, Piga M, Azzolin I, McConnell R, Iagnocco A. Rheumatoid arthritis: Extra-articular manifestations and comorbidities. Autoimmunity Reviews. 2021; 20: 102776.

[4] Cooper C, Chapurlat R, Al-Daghri N, Herrero-Beaumont G, Bruyère O, Rannou F, *et al*. Safety of Oral Non-Selective Non-Steroidal Anti-Inflammatory Drugs in Osteoarthritis: What Does the Literature Say? Drugs & Aging. 2019; 36: 15–24.

[5] Wu R, Chen F, Wang N, Tang D, Kang R. ACOD1 in immunometabolism and disease. Cellular & Molecular Immunology. 2020; 17: 822–833.

[6] Luchner M, Reinke S, Milicic A. TLR Agonists as Vaccine Adjuvants Targeting Cancer and Infectious Diseases. Pharmaceutics. 2021; 13: 142.

[7] Cao B, Chen Y, Cui J, Sun Y, Xu T. Zw10 negatively regulates the MyD88-mediated NF-κB signaling through autophagy in teleost fish. Developmental and Comparative Immunology. 2022; 132: 104401.

[8] Jia R, Cao LP, Du JL, He Q, Gu ZY, Jeney G, *et al*. Effects of high-fat diet on antioxidative status, apoptosis and inflammation in liver of tilapia (Oreochromis niloticus) via Nrf2, TLRs and JNK pathways. Fish and Shellfish Immunology. 2020; 104: 391–401.

[9] Ruan A, Wang Q, Ma Y, Zhang D, Yang L, Wang Z, *et al*. Efficacy and Mechanism of Electroacupuncture Treatment of Rabbits With Different Degrees of Knee Osteoarthritis: A Study Based on Synovial Innate Immune Response. Frontiers in Physiology. 2021; 12: 642178.

[10] Fillatreau S, Manfroi B, Dörner T. Toll-like receptor signalling in B cells during systemic lupus erythematosus. Nature Reviews. Rheumatology. 2021; 17: 98–108.

[11] Capitani M, Al-Shaibi AA, Pandey S, Gartner L, Taylor H, Hubrack SZ, *et al*. Biallelic TLR4 deficiency in humans. The Journal of Allergy and Clinical Immunology. 2023; 151: 783–790.e5.

[12] Athari SS. Targeting cell signaling in allergic asthma. Signal Transduction and Targeted Therapy. 2019; 4: 45.

[13] Silva CR, Saraiva AL, Rossato MF, Trevisan G, Oliveira SM. What do we know about Toll-Like Receptors Involvement in Gout Arthritis? Endocrine, Metabolic & Immune Disorders Drug Targets. 2023; 23: 446–457.

[14] Pyon EY. Once-monthly ibandronate for postmenopausal osteoporosis: review of a new dosing regimen. Clinical Therapeutics. 2006; 28: 475–490.

[15] Kobayakawa T, Miyazaki A, Takahashi J, Nakamura Y. Verification of efficacy and safety of ibandronate or denosumab for postmenopausal osteoporosis after 12-month treatment with romosozumab as sequential therapy: The prospective VICTOR study. Bone. 2022; 162: 116480.

[16] Klaus J, Reinshagen M, Herdt K, Adler G, von Boyen GBT, von Tirpitz C. Intravenous ibandronate or sodium-fluoride–a 3.5 years study on bone density and fractures in Crohn's disease patients with osteoporosis. Journal of Gastrointestinal and Liver Diseases. 2011; 20: 141–148.

[17] Kim JH, Jeong HE, Baek YH, Cho SW, Lim H, Shin JY. Treatment pattern in postmenopausal women with osteoporosis: a population-based cohort study in South Korea. Journal of Bone and Mineral Metabolism. 2022; 40: 109–119.

[18] Cha SM, Shin HD, Lee SH. Inevitable nonunion after ulnar shortening osteotomy in patients with ulnar impaction syndrome and breast cancer under bisphosphonate treatment. Archives of Orthopaedic and Trauma Surgery. 2020; 140: 1567–1574.

[19] Sakai S, Takeda S, Sugimoto M, Shimizu M, Shimonaka Y, Yogo K, *et al*. Treatment with the combination of ibandronate plus eldecalcitol has a synergistic effect on inhibition of bone resorption without suppressing bone formation in ovariectomized rats. Bone. 2015; 81: 449–458.

[20] Jin Z, Chang B, Wei Y, Yang Y, Zhang H, Liu J, *et al*. Curcumin exerts chondroprotective effects against osteoarthritis by promoting AMPK/PINK1/Parkin-mediated mitophagy. Biomedicine & Pharmacotherapy. 2022; 151: 113092.

[21] Jiang Y, Zhou X, Hu R, Dai A. TGF-β1-induced SMAD2/3/4 activation promotes RELM-β transcription to modulate the endothelium-mesenchymal transition in human endothelial cells. The International Journal of Biochemistry & Cell Biology. 2018; 105: 52–60.

[22] Geyer M, Schönfeld C. Novel Insights into the Pathogenesis of Osteoarthritis. Current Rheumatology Reviews. 2018; 14: 98–107.

[23] Lv Z, Yang YX, Li J, Fei Y, Guo H, Sun Z, *et al*. Molecular Classification of Knee Osteoarthritis. Frontiers in Cell and Developmental Biology. 2021; 9: 725568.

[24] Villatoro-Villar M, Kwoh CK. Bisphosphonates, Bone and Joint Pain. Current Osteoporosis Reports. 2021; 19: 417–428.

[25] Moreau M, Rialland P, Pelletier JP, Martel-Pelletier J, Lajeunesse D, Boileau C, *et al*. Tiludronate treatment improves structural changes and symptoms of osteoarthritis in the canine anterior cruciate ligament model. Arthritis Research & Therapy. 2011; 13: R98.

[26] Vassão PG, Parisi J, Penha TFC, Balão AB, Renno ACM, Avila MA. Association of photobiomodulation therapy (PBMT) and exercises programs in pain and functional capacity of patients with knee osteoarthritis (KOA): a systematic review of randomized trials. Lasers in Medical Science. 2021; 36: 1341–1353.

[27] Marchev AS, Dimitrova PA, Burns AJ, Kostov RV, Dinkova-Kostova AT, Georgiev MI. Oxidative stress and chronic inflammation in osteoarthritis: can NRF2 counteract these partners in crime? Annals of the New York Academy of Sciences. 2017; 1401: 114–135.

[28] Javaheri B, Poulet B, Aljazzar A, de Souza R, Piles M, Hopkinson M, *et al*. Stable sulforaphane protects against gait anomalies and modifies bone microarchitecture in the spontaneous STR/Ort model of osteoarthritis. Bone. 2017; 103: 308–317.

[29] Liong S, Lappas M. The Stress-responsive Heme Oxygenase (HO)-1 Isoenzyme is Increased in Labouring Myometrium where it Regulates Contraction-associated Proteins. American Journal of Reproductive Immunology. 2015; 74: 62–76.

[30] Dar QA, Schott EM, Catheline SE, Maynard RD, Liu Z, Kamal F, *et al*. Daily Oral Consumption of Hydrolyzed Type 1 Collagen Is Chondroprotective and Anti-Inflammatory in Murine Posttraumatic Osteoarthritis. PLoS ONE. 2017; 12: e0174705.

[31] Gu H, Jiao Y, Yu X, Li X, Wang W, Ding L, *et al*. Resveratrol Inhibits the IL-1β-induced Expression of MMP-13 and IL-6 in Human Articular Chondrocytes via TLR4/MyD88-dependent and -Independent Signaling Cascades. International Journal of Molecular Medicine. 2017; 39: 734–740.

[32] Liu L, Gu H, Liu H, Jiao Y, Li K, Zhao Y, *et al*. Protective effect of resveratrol against IL-1β-induced inflammatory response on human osteoarthritic chondrocytes partly via the TLR4/MyD88/NF-κB signaling pathway: an "in vitro study". International Journal of Molecular Sciences. 2014; 15: 6925–6940.

[33] Luo X, Bao X, Weng X, Bai X, Feng Y, Huang J, *et al*. The protective effect of quercetin on macrophage pyroptosis via TLR2/Myd88/NF-κB and ROS/AMPK pathway. Life Sciences. 2022; 291: 120064.

[34] Dutta D, Jana M, Majumder M, Mondal S, Roy A, Pahan K. Selective targeting of the TLR2/MyD88/NF-κB pathway reduces α-synuclein spreading in vitro and in vivo. Nature Communications. 2021; 12: 5382.

[35] Mendez ME, Murugesh DK, Sebastian A, Hum NR, McCloy SA, Kuhn EA, *et al*. Antibiotic Treatment Prior to Injury Improves Post-Traumatic Osteoarthritis Outcomes in Mice. International Journal of Molecular Sciences. 2020; 21: 6424.

[36] Mendez ME, Murugesh DK, Sebastian A, Hum NR, McCloy SA, Kuhn EA, *et al*. Antibiotic Treatment Prior to Injury Improves Post-Traumatic Osteoarthritis Outcomes in Mice. International Journal of Molecular Sciences. 2020; 21: 6424.